

Article

An RSU Deployment Scheme for Vehicle-Infrastructure Cooperated Autonomous Driving

Lingyu Zhang¹ , Li Wang¹, Lili Zhang^{2,3,*} , Xiao Zhang⁴ and Dehui Sun¹

¹ Beijing Key Lab of Urban Intelligent Control Technology, North China University of Technology, Beijing 100144, China

² College of Information Engineering, Beijing Institute of Petrochemical Technology, Beijing 102617, China

³ Xufeng Technology Co., Ltd., Yinchuan 750011, China

⁴ Hebei Vocational College of Politics and Law, Shijiazhuang 050064, China

* Correspondence: zhanglili@bipt.edu.cn

Abstract: For autonomous driving vehicles, there are currently some issues, such as limited environmental awareness and locally optimal decision-making. To increase the capacity of autonomous cars' environmental awareness, computation, decision-making, control, and execution, intelligent roads must be constructed, and vehicle–infrastructure cooperative technology must be used. The Roadside unit (RSU) deployment, a critical component of vehicle–infrastructure cooperative autonomous driving, has a direct impact on network performance, operation effects, and control accuracy. The current RSU deployment mostly uses the large-spacing and low-density concept because of the expensive installation and maintenance costs, which can accomplish the macroscopic and long-term communication functions but fall short of precision vehicle control. Given these challenges, this paper begins with the specific requirements to control intelligent vehicles in the cooperative vehicle–infrastructure environment. An RSU deployment scheme, based on the improved multi-objective quantum-behaved particle swarm optimization (MOQPSO) algorithm, is proposed. This RSU deployment scheme was based on the maximum coverage with time threshold problem (MCTTP), with the goal of minimizing the number of RSUs and maximizing vehicle coverage of communication and control services. Finally, utilizing the independently created open simulation platform (OSP) simulation system, the model and algorithm's viability and effectiveness were assessed on the Nguyen–Dupuis road network. The findings demonstrate that the suggested RSU deployment scheme can enhance network performance and control the precision of vehicle–infrastructure coordination, and can serve as a general guide for the deployment of RSUs in the same application situation.

Keywords: autonomous driving; vehicle–infrastructure coordination; human–machine driving; roadside unit



Citation: Zhang, L.; Wang, L.; Zhang, L.; Zhang, X.; Sun, D. An RSU Deployment Scheme for Vehicle-Infrastructure Cooperated Autonomous Driving. *Sustainability* **2023**, *15*, 3847. <https://doi.org/10.3390/su15043847>

Academic Editor: Shuai Su

Received: 9 December 2022

Revised: 11 February 2023

Accepted: 14 February 2023

Published: 20 February 2023



Copyright: © 2023 by the authors. Licensee MDPI, Basel, Switzerland. This article is an open access article distributed under the terms and conditions of the Creative Commons Attribution (CC BY) license (<https://creativecommons.org/licenses/by/4.0/>).

1. Introduction

The concepts of electrification, intelligence, connectivity, and sharing in the automotive industry are increasingly becoming a reality. The development of self-driving cars has recently accelerated on a global scale. Along with the growth in investments in research and development, there have been significant upticks in test, verification, and demonstrational applications. Generally speaking, according to SAE J3016 [1] and GB/T 40429 [2], Figure 1 illustrates that the L2–L3 level of self-driving car development is still being reached globally. The car is now being driven by an autonomous driving system and a human driver. The focus of conventional research is on autonomous vehicles, which are used to study how controls are switched between different types of drivers. However, barriers, poor weather, and other environmental factors can readily impair autonomous driving (AD), and there are issues with object identification, trajectory prediction, and control switch. Vehicle–infrastructure cooperated autonomous driving (VICAD) may significantly increase the perception range and perceptual ability of self-driving vehicles, achieve multi-scenario,

in-depth decision, and realize cooperative awareness and decision control—all of which contribute to the safety of AD [3].

Level	Name	Control	Monitor	Takeover	Application Scenario
L0	No Automation	Driver	Driver	Driver	/
L1	Driver Assistance	Driver System	Driver	Driver	Partial
L2	Partial Automation	System	Driver	Driver	Partial
L3	Conditional Automation	System	System	Driver	Partial
L4	High Automation	System	System	System	Partial
L5	Full Automation	System	System	System	All

Figure 1. SAE categorization standard for autonomous vehicles.

Although VICAD has evolved into a crystal-clear technology roadmap for the advancement of autonomous driving in our nation, various degrees of self-driving cars exert varying demands on the capacity of the road. At the same time, China has a vast network of highways, each of which has unique physical characteristics and cognitive requirements. Therefore, it is essential to implement intelligent road categorization, in line with VICAD growth and intelligent road building, in our nation. Research on a road classification system for vehicle–infrastructure cooperated autonomous driving is currently being conducted, both domestically and internationally [4–8]. Domestic roads have been intelligently classified in the literature [6], which has split the level of intelligence into six levels: C0–C5 (see Figure 2). In order to enhance the vision and decision-making capabilities of L2–L3 self-driving cars, it is suggested that C4–C5 high-level, intelligent highways be constructed.

Level	Name	Perception and Positioning	Network Communication	Decision-making and Control	Matched Vehicle Level
C0	No Intelligence	None	None	None	None
C1	Inferior Intelligence	None	<ul style="list-style-type: none"> • 3G, 4G • DSRC 	None	✓ L5 ✓ L4(Partial Scenarios)
C2	Primary Intelligence	None	<ul style="list-style-type: none"> • 4G • DSRC, LTE • PC5 	None	
C3	Partial Intelligence	<ul style="list-style-type: none"> • Perception of Human Vehicle Environment • Meterlevel Positioning 	<ul style="list-style-type: none"> • 4G, 5G • DSRC, LTE • PC5 • 500ms End to End Delay 	None	
C4	High Intelligence	<ul style="list-style-type: none"> • Total Factor Perception • Multi-feature Accurate Recognition • Decimeter level Positioning 	<ul style="list-style-type: none"> • 5G Uu • LTE-V2X, NR-V2X • 200ms End to End Delay 	Partial Scenarios	✓ L2+ ✓ L3 ✓ L4 ✓ L5
C5	Full Intelligence	<ul style="list-style-type: none"> • Ubiquitous Perception • Centimeter level Positioning 	<ul style="list-style-type: none"> • 5G, NR-V2X, 6G • 100ms End to End Delay 	All Scenarios	

Figure 2. Norms for road intelligence categorization.

Since it interacts with vehicles, provides road environment information for vehicles and pedestrians, supports driving decision-making with information [9], and aids in the

networking and communication of the vehicular ad-hoc network (VANET) [10], the RSU has emerged as a crucial area of research at this time. The RSU deployment strategy is a research hotspot in addition to the RSU function study. The implementation of RSUs is limited by many factors, such as network topology, geographic location, cost, and other factors. RSU deployment plans are typically examined from a variety of angles in actual RSU deployment research for various scenarios and performance requirements. Relevant research primarily focuses on performance-optimization RSU deployment and cost-reduction RSU deployment, according to various optimization objectives.

The overall cost of RSU deployment is often predetermined by studies on performance-optimization RSU deployment, and on this foundation, the RSU deployment scheme with the best performance is developed. Maximum coverage [11–16], optimum connection [17–22], and minimal transmission latency [23–27] are the major optimization objectives. The RSU's position determines whether it can cover sufficient numbers of vehicles and other road infrastructures to prevent interruptions in information transmission. Therefore, VANET's communication performance improves as coverage increases. The term "RSU deployment with maximum coverage" refers to providing the most coverage for a certain total cost while still providing the highest amount of service to the cars on the road network. In order to address the issue of the deployment position of number-limited RSUs in an urban VANET being difficult to determine, Jia et al. developed a Dijkstra-based 0–1 covering matrix computation algorithm [11]. The method transforms vehicle coverage into split sub-road coverage in the deployment region, and a suggested RSU deployment scheme, based on an enhanced genetic algorithm, is based on this algorithm. Increasing the connection can boost the performance of network transmissions since it is one of the key performance indicators used to gauge network transmission and service. To increase the VANET connection in highway settings, Mousa et al. proposed a cost-effective deployment of RSUs [20]. They provided a generic model based on empirical data that stipulates the minimal number of candidate RSUs and their needed placements to maintain the continuous connectivity of a particular section of the roadway. RSUs can shorten the time it takes for data to be transmitted between intelligent vehicles by using vehicle-to-infrastructure (V2I) connectivity. The major goal of the research on data communication delay is to decrease RSU–RSU and vehicle–RSU communication delays. Ghorai et al. conducted research on the deployment of RSUs to minimize communication delay and came to the conclusion that placing RSUs in congested areas is the key to achieving full coverage. As a result, they proposed an RSU deployment strategy based on the constrained Delaunay triangulation method, and they obtained the optimal RSU locations through the optimization procedure and reduced communication delay in the vehicle-to-infrastructure environment [23].

Cost-minimization RSU implementation reduces costs while still fulfilling network performance requirements. The installed number and coverage areas of RSUs are immediately reduced by the low deployment costs, but they still need to provide certain network services. By including a problem-dependent encoding and unique mutation operator, as well as taking the quality of service and cost objectives into consideration, Massobrio et al. created a particular multi-objective evolutionary algorithm to investigate a set of potential RSU sites [28]. In order to reduce the total cost of capital expenditures and operational expenditures, Nikookaran et al. took into account the problem of RSU placement [29]. The minimum cost placement was first calculated using an integer linear program formulation based on the input traffic traces and candidate sites. An innovative and effective RSU deployment problem model was developed by Gao et al. It consists of two models: a road network model and a profit model. The road network model supported difficult road shapes while taking into account important influencing elements, such as the number of lanes and popularity [30].

In the current RSU deployment schemes, the hotspot deployment method—in which RSUs are positioned at traffic crossings, crowded areas, or accident-prone areas—is largely used due to the high cost of RSU deployment. The biggest benefit of this method is that it is inexpensive to deploy and maintain, allowing for simple communication functionality

between vehicles and RSUs as well as the provision of long-term and macroscale traffic information services for vehicles. However, it is challenging to implement precise control for vehicles and roads. As a result, it is essential to begin with the information exchange, collaboration, cooperative perception, and decision-making of VICAD before moving on to study the deployment of RSUs with a compact footprint and high density in the road network. With the aim of decreasing the number of RSUs and maximizing vehicle coverage of communication and control services, the RSU deployment topology model has been designed.

The rest of this essay is structured as follows: With the aim of reducing the number of RSUs and increasing vehicle coverage of communication and control services, Section 2 suggests an RSU deployment strategy. The self-created open simulation platform's Nguyen-Dupuis simulation road network model is produced in Section 3, where experimental findings are provided. The summary of conclusions and planned work is presented in Section 4.

2. Materials and Methods

2.1. Road Network Model

In this research, it is assumed that all RSUs have circular communication coverage and the same communication radius, which is R , for the urban road network or expressway network in the vehicle–infrastructure cooperative environment. Within its communication range, the RSU can talk to cars or other RSUs. The communication between the vehicle and the RSU, however, occasionally extends outside of one RSU's communication coverage area. Typically, the road's width is disregarded because the RSU's communication radius is significantly greater than it is. The communication between cars is not taken into account in this article, and to make the issue more simplified, the network communication environment of the uplink between the RSU and the vehicle is not taken into account. RSUs are typically placed in certain areas with significant spatial characteristics, such as road intersections, because they not only offer better data distribution [31] but also have the potential to increase RSU communication coverage by 15% [32]. Road intersections are, therefore, given priority in this research as potential deployment sites for RSUs.

Before deploying RSUs, the road network should be abstracted into a mathematical model. Planar undirected graphs are a popular method. $G = (V, E)$ represents a graph with vertex set, V , and edge set, E . V denotes the set of RSU candidate deployment positions, with $V = \{V_1, V_2, \dots, V_x\}$ and $|V| = x$. E is the set of links connecting RSU candidate deployment positions, $E = \{E_1, E_2, \dots, E_y\}$, and $D = \{D_1, D_2, \dots, D_y\}$ is the set of link lengths. Further segmentation is performed for the link E_k with $D_k \in D$ and $D_k > 2R$, and $\lceil (D_k - L)/L \rceil$ new nodes of equal length L are inserted into the link [33], which are used as candidate deployment positions of RSUs to maximize the road network coverage and achieve accurate control of vehicles and roads. Let $G' = (V', E')$ be an undirected graph with segmented links. $V' = \{V, N\}$, $|V'| = m$ and N is the node set formed when $E \in G = (V, E)$ is segmented, $N = \{N_1, N_2, \dots, N_z\}$. $E' = \{e(i, j), \forall i, j, i \in V', j \in V'\}$, $|E'| = p$, and $e(i, j) = \{l_{ij}, \rho_{ij}, v_{ij}\}$. Use the road network in Figure 3 with $x = 12$ as a starting point, and apply the mathematical model to abstract it to create the undirected graph in Figure 4.

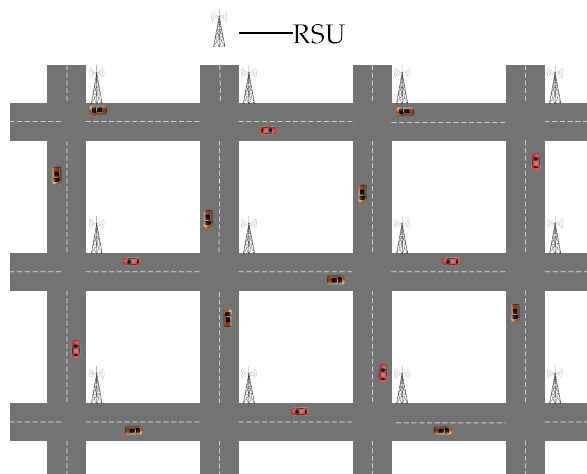


Figure 3. The diagram of the road network.

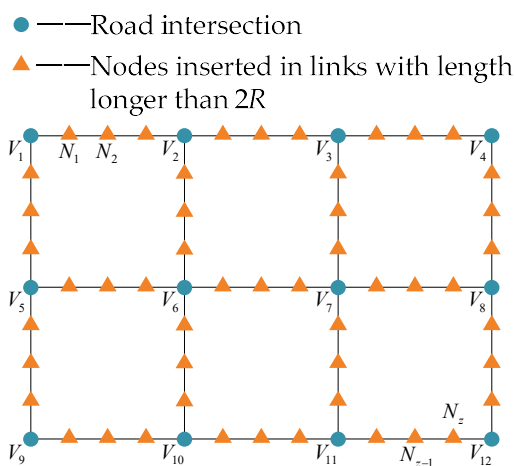


Figure 4. The diagram of the road network represented by an undirected graph.

2.2. Time Threshold

This study uses MCTTP to build an RSU deployment scheme in the road network [13]. C stands for the collection of cars in the road network and has the following value $C = \{C_1, C_2, \dots, C_n\}$. Let's say there is an $m \times n$ matrix $\mathbf{T} = (t_{ab})$, where the element $t_{ab} (1 \leq a \leq m, 1 \leq b \leq n, t_{ab} \geq 0)$ reflects the amount of time that vehicle C_b spends within the RSU's communication coverage area that is deployed at V'_a over a certain period of time. Let τ_1 represent the minimal amount of time needed for the vehicle to effectively connect to and communicate with the RSUs. Since the communication between the RSU and the vehicle can be completed through several RSUs, it can be said that vehicle C_b can be served by communication if the total time it spends in each RSU's communication coverage area during this period is larger than τ_1 .

The RSU serves as the primary point of information exchange in the vehicle–infrastructure cooperative environment. It not only sends and receives traffic information in real-time, but it also carries out the task of transmitting the cloud control platform's control instructions to autonomous driving vehicles, such as issuing the local high-resolution map on specific road sections, controlling the switch between driving subjects in specific scenes, and re-planning traffic. As a result, the RSU should communicate time-sensitive control commands, meaning they can only be executed by the vehicle within a particular window of time after connecting to the RSU. Assume that the $m \times m$ matrix $\mathbf{T}_d = (t_{ij}^d)$ has an element, $t_{ij}^d = (a \leq i \leq m, a \leq j \leq m, t_{ij}^d \geq 0)$, which reflects the amount of time that the vehicle,

$C_d (C_d \in C_b)$, spends traveling across the link, $e(i,j)$, over the course of a certain period of time.

Let τ be the maximum amount of time needed from the time the vehicle connects to the RSU to when it successfully receives a specific control instruction because the time to accomplish the driving task or control command is not fixed. It is given that the vehicle can only successfully receive control commands when it is in successful communication with the RSUs. The equation for the relationship between τ and τ_1 is $\tau = \tau_1 + \tau_2$, where τ_2 is the entire amount of time the vehicle spends on the link, $e(i,j)$, during the time that it successfully connects to the RSU and communicates. It is assumed that vehicle C_d can be served by control if the time it takes for it to successfully receive a control command is less than τ within a given time frame.

For instance, in a particular amount of time, we obtain the 8×6 matrix \mathbf{T} :

$$\mathbf{T} = \begin{bmatrix} 7 & 10 & 10 & 0 & 0 & 6 \\ 0 & 7 & 7 & 0 & 0 & 3 \\ 0 & 9 & 12 & 0 & 0 & 0 \\ 7 & 0 & 2 & 6 & 0 & 6 \\ 0 & 2 & 0 & 0 & 5 & 0 \\ 8 & 0 & 0 & 11 & 9 & 8 \\ 7 & 0 & 0 & 6 & 8 & 0 \\ 5 & 0 & 0 & 10 & 6 & 0 \end{bmatrix}$$

The matrix \mathbf{T} indicates that there are 8 RSUs in this road network and that 6 vehicles pass through within the given time. The period that these 6 vehicles spend within the RSUs' communication coverage area can be determined to be 34 s, 28 s, 35 s, 33 s, 28 s, and 23 s, respectively. Only the vehicles C_1 , C_3 , and C_4 can be served by communication if $\tau_1 = 30$ s.

The traffic scenario (see Figure 5) was built in accordance with the matrix, \mathbf{T} . There are four road intersections in this picture and their distances are more than $2R$. The image illustrates how vehicles C_1 , C_3 , and C_4 remain outside the RSU's communication coverage area during the time they successfully connect to and interact with the RSU, allowing for the determination of the matrices \mathbf{T}_1 , \mathbf{T}_3 , and \mathbf{T}_4 . It can be determined that these 3 cars took 52 s, 47 s, and 46 s, in the appropriate order, between connecting to the RSU and successfully receiving a particular control command. Only the vehicles C_3 and C_4 can be served by control during this time if $\tau = 50$ s.

$$\mathbf{T}_1 = \begin{bmatrix} 0 & 0 & 0 & 0 & 0 & 0 & 0 & 0 \\ 0 & 0 & 0 & 3 & 0 & 0 & 0 & 0 \\ 0 & 0 & 0 & 0 & 0 & 0 & 0 & 0 \\ 0 & 0 & 0 & 0 & 0 & 4 & 0 & 0 \\ 0 & 0 & 0 & 0 & 0 & 0 & 0 & 0 \\ 0 & 0 & 0 & 0 & 0 & 0 & 5 & 0 \\ 0 & 0 & 0 & 0 & 0 & 0 & 0 & 6 \\ 0 & 0 & 0 & 0 & 0 & 0 & 0 & 0 \end{bmatrix} \quad \mathbf{T}_3 = \begin{bmatrix} 0 & 4 & 0 & 0 & 0 & 0 & 0 & 0 \\ 0 & 0 & 5 & 0 & 0 & 0 & 0 & 0 \\ 0 & 0 & 0 & 0 & 3 & 0 & 0 & 0 \\ 0 & 0 & 0 & 0 & 0 & 0 & 0 & 0 \\ 0 & 0 & 0 & 0 & 0 & 0 & 0 & 0 \\ 0 & 0 & 0 & 0 & 0 & 0 & 0 & 0 \\ 0 & 0 & 0 & 0 & 0 & 0 & 0 & 0 \\ 0 & 0 & 0 & 0 & 0 & 0 & 0 & 0 \end{bmatrix} \quad \mathbf{T}_4 = \begin{bmatrix} 0 & 0 & 0 & 0 & 0 & 0 & 0 & 0 \\ 0 & 0 & 0 & 0 & 0 & 0 & 0 & 0 \\ 0 & 0 & 0 & 0 & 0 & 0 & 0 & 0 \\ 0 & 0 & 0 & 0 & 0 & 0 & 0 & 0 \\ 0 & 0 & 0 & 0 & 0 & 0 & 0 & 0 \\ 0 & 0 & 0 & 2 & 0 & 0 & 0 & 0 \\ 0 & 0 & 0 & 0 & 0 & 7 & 0 & 0 \\ 0 & 0 & 0 & 0 & 0 & 0 & 4 & 0 \end{bmatrix}$$

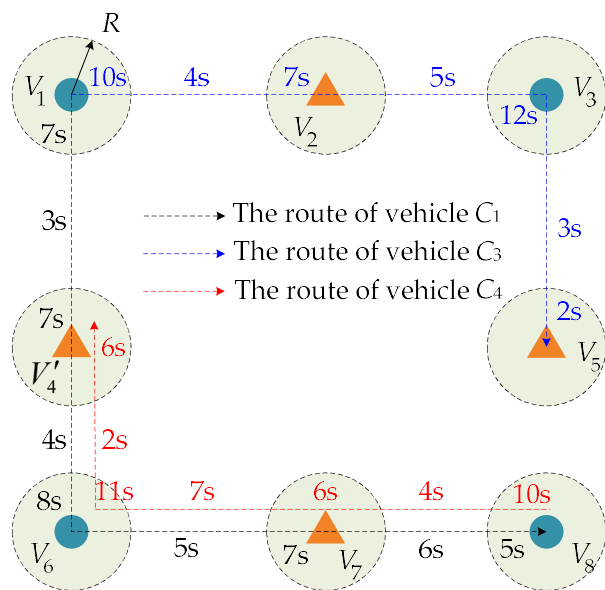


Figure 5. The route taken by vehicles.

2.3. Objectives

When enough RSUs are installed, road segments may be fully covered, which eliminates the issue of communication and control time limits between RSUs and cars and enhances the effectiveness of operations and the control precision of vehicle–infrastructure coordination. However, because RSU installation and maintenance costs are high, and in the dense RSU deployment scheme, communication between RSUs will interfere with each other and degrade network performance. As a result, the goal of this paper was to deploy as few RSUs, as possible, in order to provide communication and control services to a greater number of vehicles. The amount of RSUs deployed is dependent on how far apart new nodes are, which are divided into road segments. The issue can be reduced to choosing a long L to maximize the RSU coverage area and creating the following maximized multi-objective optimization function.

$$\max f_1 = \frac{1}{m} \tag{1}$$

$$f_2 = \frac{|C_s|}{n} \times 100\% \tag{2}$$

$$f_3 = \frac{|C_r|}{|C_s|} \times 100\% \tag{3}$$

$$\text{s.t. } t(C_b) = \sum_a^m t_{ab} > \tau_1, C_b \in C_s, C_s \in C \tag{4}$$

$$t(C_d) = \sum_a^m \sum_a^m t_{ij}^d, C_d \in C_r, C_r \in C_s \tag{5}$$

$$t(C_b) + t(C_d) < \tau, C_b \in C_r, C_d \in C_r \tag{6}$$

The reciprocal of the number of RSUs deployed in the road network is represented by f_1 in Formula (1); the higher its value, the fewer RSUs must be placed on the road network. Formula (2) states that C_s stands for the set of vehicles that can be served by communication, and $|C_s|$ is the total number of vehicles that can be served by communication during the time period indicated. Formula (4)'s constraint condition, where $t(C_b)$ is the entire amount of time that vehicle C_b spent in the communication coverage area of the RSUs is used to describe the vehicle coverage rate of communication service during this time. It is assumed that communication can serve the vehicle C_b if $t(C_b) > \tau_1$. Formula (3) states

that C_r is the set of vehicles that can be served by control, and $|C_r|$ is the entire number of vehicles that can be served by communication within a given period. f_3 represents the vehicle coverage rate of control services within this period, and its constraint condition is as shown in Formulas (5) and (6), where $t(C_d)$ is the total amount of time that vehicle C_d spends passing through the link, $e(i,j)$, during the time when it successfully connects to and communicates the RSU. If $t(C_b) + t(C_d) < \tau$, then it is assumed that the vehicle, C_d , can be served by communication.

2.4. Method

The optimization problem for RSU deployment that is put forth in this study is a multi-objective optimization problem (MOP). Numerous techniques have been suggested in recent research to solve the MOP's optimal solution set [34]. Due to its straightforward idea, great efficiency, quick speed, and ease of implementation, particle swarm optimization (PSO) [35] has produced positive outcomes when tackling different MOPs in scientific study and real-world engineering. Since Coello and Lechuga [36] initially introduced it in 2002, people have learned from the multi-objective evolutionary algorithm to address the limitations of the multi-objective particle swarm optimization (MOPSO) algorithm [37]. Quantum-behaved particle swarm optimization (QPSO) [38] fixes the flaw that prevents PSO from searching the whole possible search space.

The QPSO only has the displacement update, for which the update equation is as follows [38], while the PSO retains the velocity update.

$$X_{i,j}(k) = p_{i,j}(k) \pm \alpha |mbest_j(k) - X_{i,j}(k)| * \ln \frac{1}{u_{i,j}(g)} \quad (7)$$

$$p_{i,j}(k) = \varphi_j(k) * pbest_{i,j}(k) + [1 - \varphi_j(k) * gbest_j(k)] \quad (8)$$

$$\begin{aligned} mbest &= (mbest_1, mbest_2, \dots, mbest_Q) = \frac{1}{P} \sum_{i=1}^P pbest_i \\ &= \left(\frac{1}{P} \sum_{i=1}^P pbest_{i,1}, \frac{1}{P} \sum_{i=1}^P pbest_{i,2}, \dots, \frac{1}{P} \sum_{i=1}^P pbest_{i,P} \right) \end{aligned} \quad (9)$$

where, we denote, by $i(i = 1, 2, \dots, P)$, the i th particle; by P , the population size; by $j(j = 1, 2, \dots, Q)$, the particle's dimension; by Q , the search space's dimension; by k , the evolutionary generation. Both $u_{i,j}(g)$ and $\varphi_j(k)$ are random numbers uniformly distributed on the interval. $X_{i,j}(k)$, $p_{i,j}(k)$, and $pbest_{i,j}(k)$ are, respectively, the current position, attractor position, and individual best position of the j th-dimension particle, i , in the k th generation. $gbest_j(k)$ is the global best position of the j th-dimension particles in the k th generation. $mbest_j(k)$ is the average best position of the j th-dimension particles in the k th generation, which is defined as the average of the individual best positions of all particles. The only parameter of QPSO, besides population size and evolutionary generation, is known as the expansion-contraction factor, α . The algorithm may be assured to converge when $\alpha < 1.782$, according to simulation results in the literature [39]. Typically, as the number of evolutionary generations rises, the value will gradually drop from 1.0 to 0.5.

The variety of solution sets cannot be guaranteed by QPSO's quick convergence rate because it is prone to converge prematurely. This study establishes an external archive to keep the non-inferior solutions discovered throughout the search process in order to swiftly approach the Pareto-optimal frontier, referring to the diversity maintenance method in literature [39]. The MOQPSO solution set is kept diverse by using the crowding distance ranking mechanism in non-dominated sorting genetic algorithm II (NSGA-II) [40].

(1) The selection of the global best position

Due to the limits placed on each objective, it is challenging to solve MOPs while simultaneously optimizing several objectives. As a result, we can only weigh the competing objectives to provide an optimal solution set that includes a variety of elements. To do this, the particles in the external archive are updated after each generation, and a suitable $gbest$

is chosen for each particle using the crowding distance approach. The literature is cited for the specific calculating approach [40]. The binary tournament selection technique, based on the crowding distance value, selects *gbest* for each particle in the external archive after first computing the crowding distance value for all particles in the external archive. The likelihood of the particle being chosen as the *gbest* increases with the crowding distance value because the particle is spread more uniformly in the target space.

(2) Mutation operator

In order to retain the diversity of solutions during the search process, the mutation operator is incorporated into the MOQPSO when solving MOPs because the quick convergence speed of QPSO is prone to converge prematurely. The unique method is that the mutation operator applies to all particles in the early stages of seeking optimization. The mutation operator's function is diminished as evolutionary generation increases, which is mostly reflected in the decline in mutation probability and mutation range, meaning that it only applies to some particles in the midst of search optimization. There is no longer any mutation in the later stage, enabling a fine search for particles in the final solution region. Given that irregular random mutation can lead to degradation, the local search ability of the Gaussian mutation can help to improve the algorithm's local search accuracy. As a result, in this paper, the random mutation method with Gaussian distribution characteristics was chosen.

(3) The updated policy of the external archive

When an updated particle dominates one or more particles in the external archive, an update to the external archive is necessary. Additionally, since the external archive has a size restriction and the number of non-inferior solutions will grow as searching optimization progresses, it is required to develop an update mechanism to prune the external archive at this time. The crowding distance method is used to update the external archive's particles when the number of particles reaches its maximum capacity. This method keeps the most uniformly distributed and largest crowding distance-valued particles, which effectively preserves the diversity of the external archive's particles.

(4) The MOQPSO installation process steps

The following are the precise steps of the MOQPSO algorithm based on the crowding distance approach.

Step 1: Set the basic parameters of the algorithm, initialize all particles in the search space, and define the initial *pbest_i* of each particle as the initial position of the particle;

Step 2: Assess each particle in the particle swarm, and, using the Pareto-dominance relation, place the non-inferior solutions in the external archive;

Step 3: Choose the *gbest* for every particle in the particle swarm, modify each particle's position in accordance with equations (7)~(9), and mutate using the random mutation method with Gaussian distribution properties;

Step 4: Re-evaluate each particle in the particle swarm and update each particle's best individual position, *pbest*. The upgraded particle is regarded as the new *pbest* if it outperforms *pbest*. One of them is chosen at random to become the new *pbest* if they do not outperform one another;

Step 5: Apply the crowding distance method to update the particles in the external archive;

Step 6: Determine if the present evolutionary generation has evolved to its full potential; if so, move on to Step 8; otherwise, move on to Step 3;

Step 7: Export every particle to the external archive as the complete answer.

3. Results and Evaluations

We carried out the experiments and comparisons with the traditional algorithms, the multi-objective objective firefly algorithm (MOFA) [41] and the MOPSO [36], in order to validate the suggested approach. The Nguyen–Dupuis road network model [42] was used

as the experimental input data, and it was built in the OSP [43]. We then extracted the vehicle trajectory data produced through simulation within an hour, including time stamps, vehicle IDs, map coordinates of vehicles, instantaneous vehicle velocities, and other data. The road network topology (see Figure 6) and the simulation road network model (see Figure 7) were created in the OSP of Nguyen–Dupuis, respectively. The road network consisted of 13 intersections (A–M), 19 internal links (1–19), and 4 input and output links (Q_1 – Q_4), and each link's length (in m) was 1800, 1400, 1400, 2800, 1800, 600, 1000, 1000, 2400, 1800, 2600, 1800, 1800, 2000, 1200, 1800, 1800, 1000, and 2200.

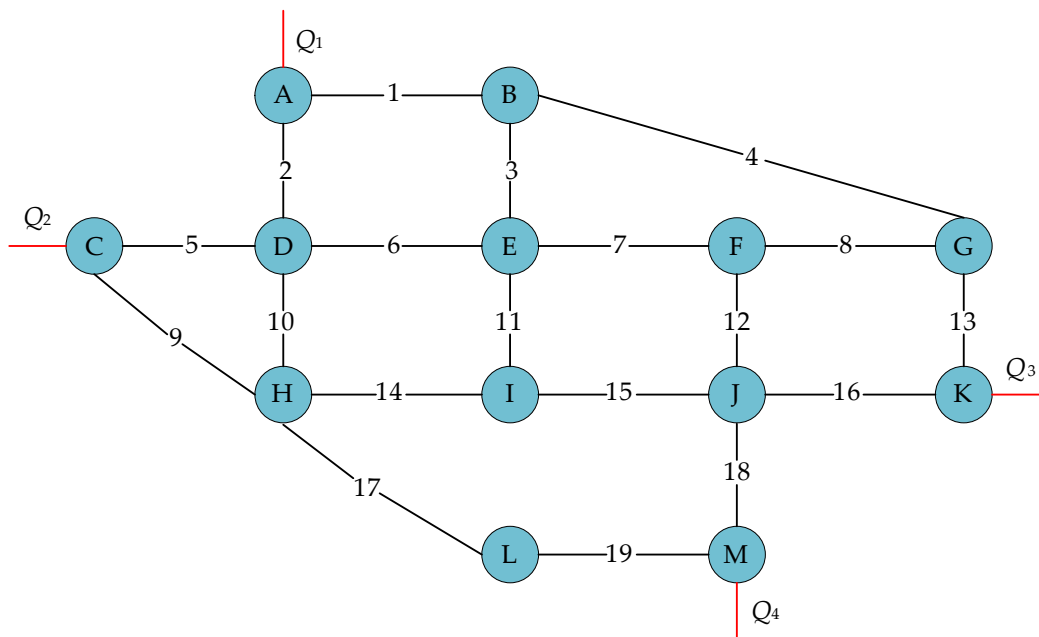


Figure 6. Nguyen–Dupuis road network topology.



Figure 7. Nguyen–Dupuis' simulation road network model.

The RSU deployment spacing, L , in this simulation scenario had a value range of 0–2800 and was an integer. The corresponding relationship between deployment spacing and the number of RSUs was provided according to the length of each link to make the future analysis of simulation results easier (see Table 1).

Table 1. The RSU count and deployment interval.

Serial No.	L/km	m	Serial No.	L/km	m
1	2.8	13	11	[0.8, 0.87)	45
2	[1.8, 2.8)	18	12	[0.74, 0.8)	46
3	[1.4, 1.8)	25	13	[0.7, 0.74)	47
4	[1.3, 1.4)	28	14	[0.67, 0.7)	50
5	[1.2, 1.3)	29	15	[0.65, 0.67)	51
6	[1.1, 1.2)	31	16	[0.6, 0.65)	52
7	[1.0, 1.1)	32	17	[0.56, 0.6)	62
8	[0.94, 1.0)	36	18	[0.55, 0.56)	63
9	[0.9, 0.94)	37	19	[0.51, 0.55)	64
10	[0.87, 0.9)	44	20	(0, 0.51)	≥65

The simulation experiment’s RSU communication radius was set at $R = 200$ m, and the threshold times were set to $\tau_1 = 30$ s and $\tau = 90$ s after thorough consideration of aspects such as the deployment economics of RSUs and the control demand of VICAD. The population size was set at 60 and the number of iterations was set at 200 to assure the fairness of the comparison findings of each algorithm. For each method, a random set of RSU layout deployment schemes was created as the initial solution, and the solution that was closest to the origin in the Pareto-optimal solution set was chosen as the best one in each iteration. Figure 8 displays the set of Pareto-optimal solutions for each algorithm. The MOQPSO algorithm provided the greatest results, which attained 97.3% of the vehicle coverage rate for communication service and 80.5% of the vehicle coverage rate for control service when 32 RSUs were installed, as can be seen from the figure.

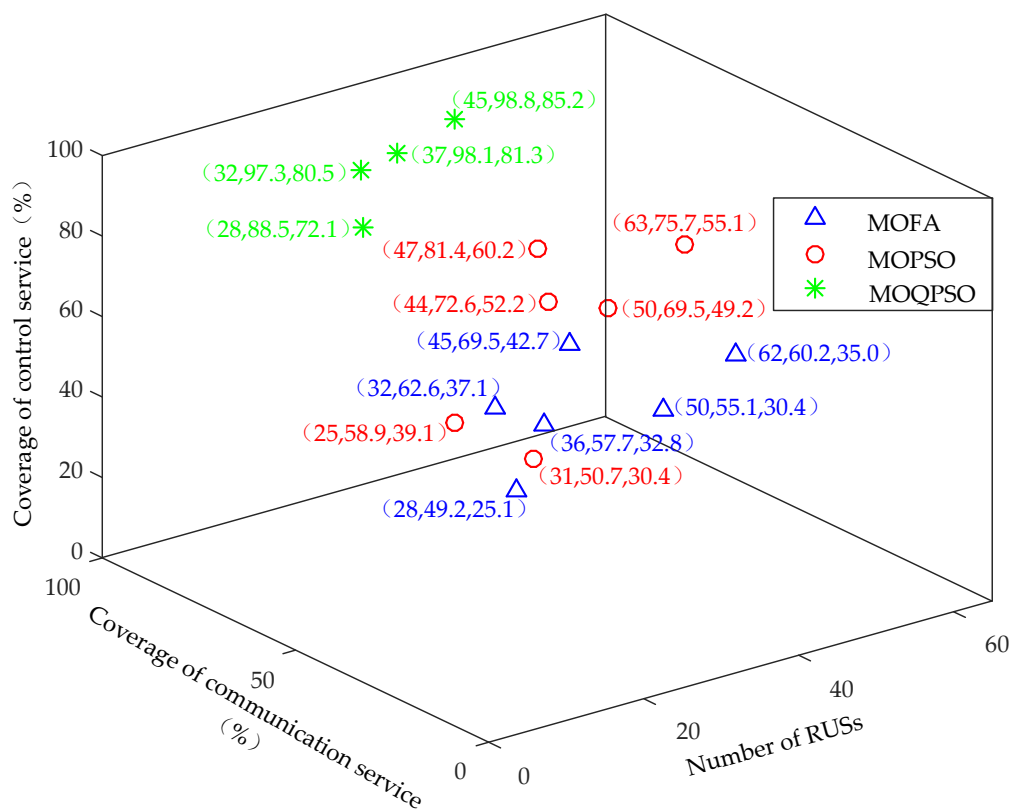
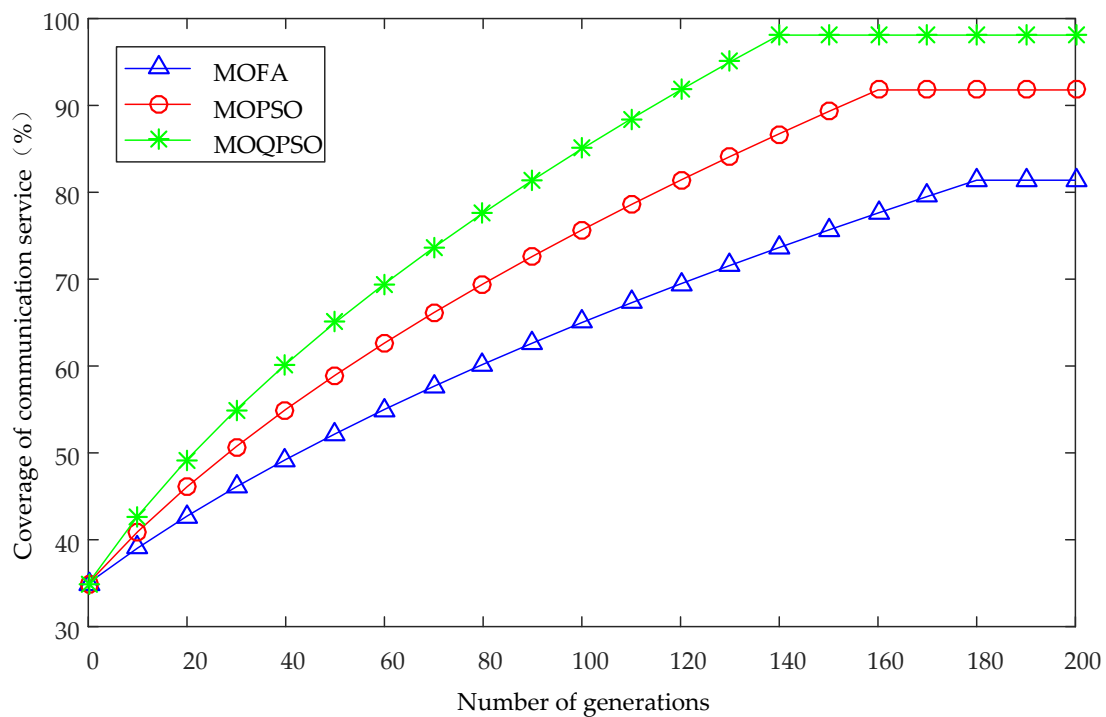


Figure 8. Each algorithm’s collection of Pareto-optimal solutions.

The convergence curves for each algorithm are displayed in Figure 9. The figure shows that the MOQPSO algorithm had the quickest rate of convergence, finishing up about 140 generations. At around 160 and 180 generations into their respective iterations, the MOPSO and MOFA algorithms reached their point of convergence. Additionally, the MOQPSO algorithm had a higher vehicle coverage rate of communication and control services when compared to the MOPSO and MOFA algorithms.

$m = \{18,25,31,36,44,50,62\}$ was chosen to assess the link between the average vehicle coverage of communication and control services and the number of RSUs under the solution of the MOQPSO algorithm in order to further determine the best value range of RSU deployment spacing, L (see Figure 10). Figure 10 demonstrates that when 31 RSUs were deployed, the vehicle coverage of the communication service was over 90% and the vehicle coverage of the control service was above 75%, resulting in a comparatively optimal effect. The vehicle coverage of the communication and control service did not greatly expand when there were more than 44 RSUs, though. The best value range of RSU spacing could be calculated as 800 m and 1200 m by using the relationship between the deployment spacing and the number of RSUs in Table 1.



(a)

Figure 9. Cont.

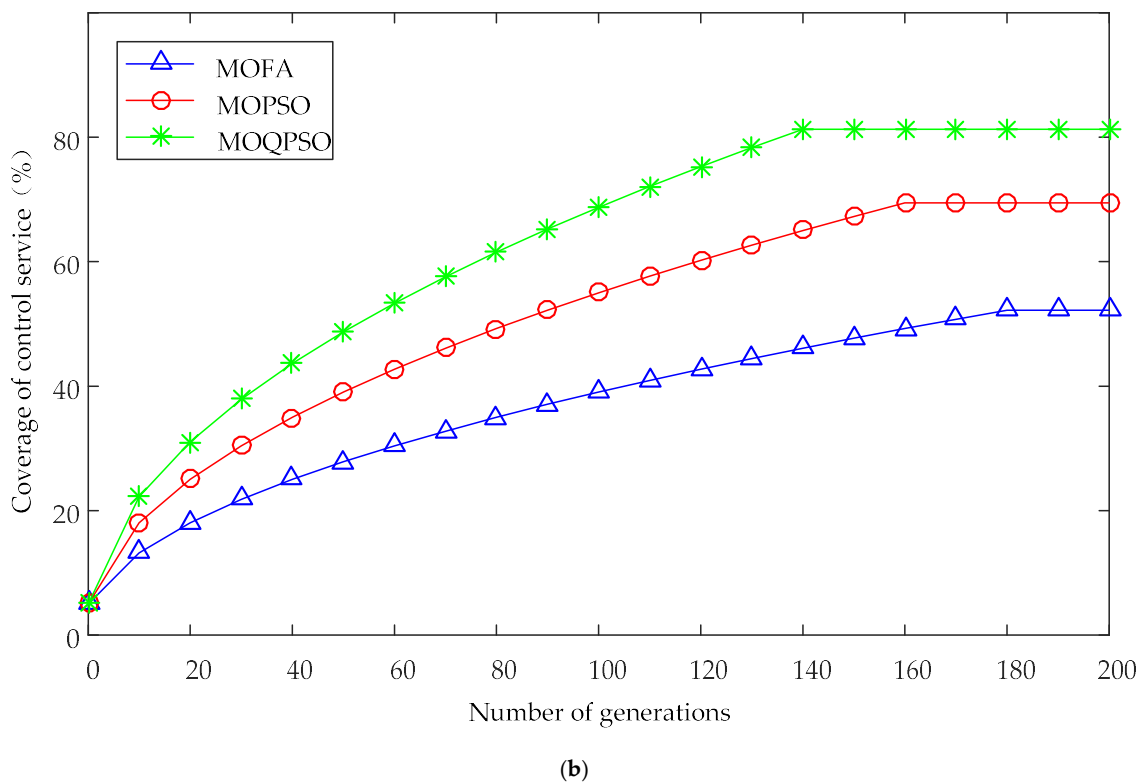


Figure 9. The convergence curves of each algorithm. (a) Coverage of communication service; (b) coverage of control service.

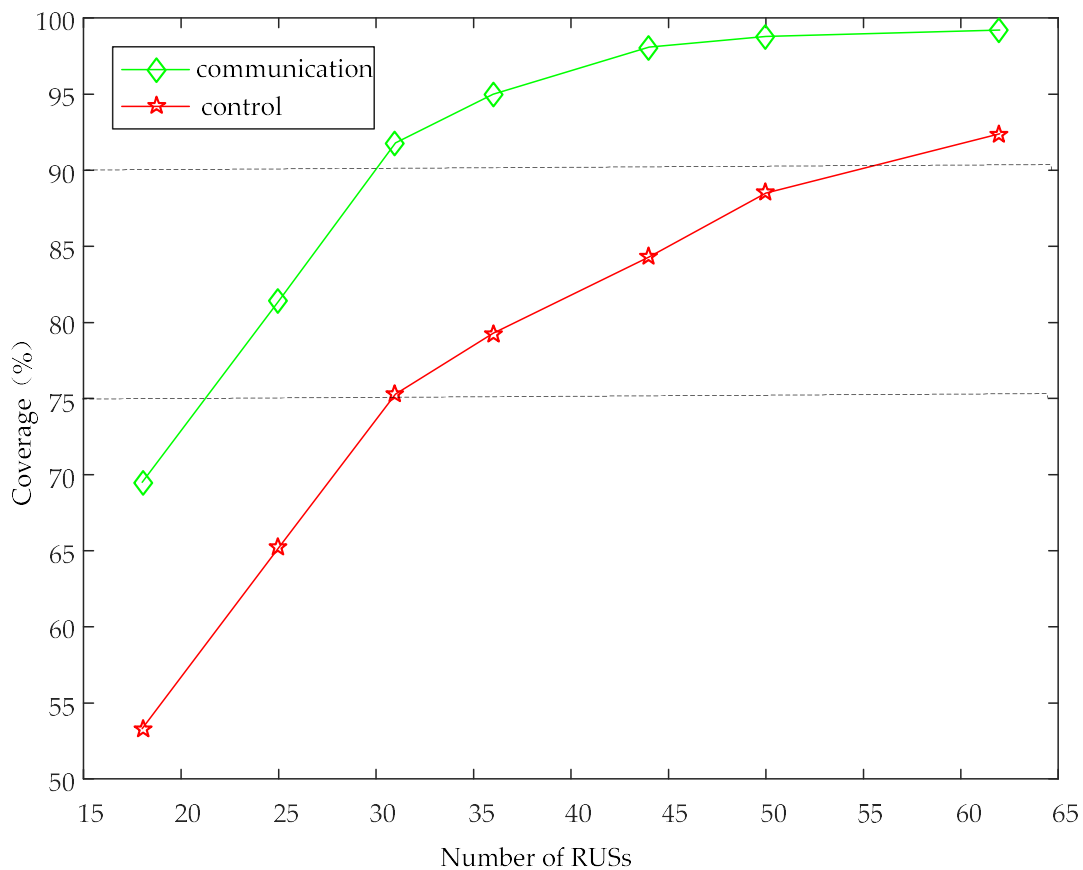


Figure 10. Average vehicle coverage at various RSU counts.

4. Discussion

The problem of RSU deployment for VICAD was investigated in this work, and using MCTTP, a certain number of RSUs were deployed to optimize vehicle coverage for the shortest possible communication time and the longest possible RSU/vehicle command receiving time. To reduce the number of RSUs deployed and increase vehicle coverage of the communication and control services, a multi-objective optimization model was built. An enhanced MOQPSO, algorithm-based, RSU deployment method was suggested to estimate the ideal RSU deployment spacing in order to address this issue. Using the experimental data, we constructed the Nguyen–Dupuis simulation road network model in the self-developed OSP and identified the best value range for RSU deployment spacing. The suggested RSU deployment plan should eventually be examined using data on vehicle trajectories from the real road network.

Author Contributions: Conceptualization, L.Z. (Lingyu Zhang) and L.Z. (Lili Zhang); methodology, L.W. and L.Z. (Lingyu Zhang); software, X.Z. and L.Z. (Lili Zhang); validation, L.W., L.Z. (Lingyu Zhang), and L.Z. (Lili Zhang); resources, L.Z. (Lingyu Zhang); data curation, X.Z.; writing—original draft preparation, L.Z. (Lingyu Zhang); writing—review and editing, D.S. and L.W.; visualization, L.Z. (Lili Zhang); supervision, D.S.; funding acquisition, L.W. All authors have read and agreed to the published version of the manuscript.

Funding: This research was supported by grants from the Beijing Municipal Science and Technology Plan (Z221100008122006), Natural Science Foundation of Ningxia (2022AAC03757), Cross-Disciplinary Science Foundation from Beijing Institute of Petrochemical Technology (BIPTCSF-006), Key Project of University-level Education and Teaching Reform and Research of Beijing Institute of Petrochemical Technology (ZD202103001), Young Talents Promotion Project of Beijing Association for Science and Technology, and Open Project for Beijing Urban Governance Research Base of North China University of Technology (21CSZL34). The referees' valuable suggestions are greatly appreciated.

Institutional Review Board Statement: The study was conducted in accordance with the Declaration of Helsinki, and approved by the Institutional Review Board (or Ethics Committee) of North China University of Technology (2022-1-02, 28 January 2022) approved the study.

Informed Consent Statement: Not applicable.

Data Availability Statement: The related authors are willing to provide the data used to support the study's findings upon request, but only for research purposes. Informed consent was obtained from all subjects involved in the study.

Conflicts of Interest: The authors declare that they have no conflict of interest.

References

1. SAE J3016. Taxonomy and Definitions for Terms Related to Driving Automation Systems for On-Road Motor Vehicles, Society of Automotive Engineers International, USA. 2021. Available online: https://www.sae.org/standards/content/j3016_202104/ (accessed on 2 July 2021).
2. GB/T 40429. Taxonomy of Driving Automation for Vehicles, Ministry of Industry and Information Technology, China. 2021. Available online: <https://openstd.samr.gov.cn/bzgk/gb/newGbInfo?hcno=4754CB1B7AD798F288C52D916BFECA34> (accessed on 6 October 2021).
3. Wang, K.; Zhang, Z.H.; Yang, F.; Hu, X.; Zhou, G.Y. Key Technology of Vehicle-Infrastructure Coordination for High-level Autonomous Driving. *Mob. Commun.* **2021**, *45*, 69–76.
4. The European Road Transport Research Advisory Council (ERTRAC). Connected Automated Driving Roadmap, Europe. 2019. Available online: <https://www.ertrac.org/wp-content/uploads/2022/07/ERTRAC-CAD-Roadmap-2019.pdf> (accessed on 7 July 2021).
5. SAE J3216. Taxonomy and Definitions for Terms Related to Cooperative Driving Automation for On-Road Motor Vehicles, Society of Automotive Engineers International, USA. 2020. Available online: https://www.sae.org/standards/content/j3216_202107/ (accessed on 8 November 2021).
6. Institute for AI Industry Research, Tsinghua University (AIR), Baidu Apollo. Key Technology and Prospect of Vehicle-Infrastructure Coordination for Autonomous Driving, China. 2021. Available online: <https://pan.baidu.com/s/1moPrX OXMzBQfA89eRgWqOQ?pwd=32W5> (accessed on 25 December 2021).

7. Autonomous Driving Working Committee of China Highway and Transportation Society. Classification and Definition for Connected Automated Highway (CAH) Systems, China. 2021. Available online: http://www.chts.cn/module/download/download_file.jsp?classid=0&filename=8271b114bea6483c9af6d0e44eb0186e.pdf (accessed on 18 December 2021).
8. Xiong, W.H.; Hu, S.P.; Wang, P.; Zhang, J.H. Research of roadside traffic facilities system and road classification in vehicle infrastructure synergistic environment. *Highway* **2022**, *67*, 218–222.
9. Ran, B.; Tan, H.C.; Zhang, J.; Qu, X. Development status and trend of connected automated vehicle highway system. *J. Automot. Saf. Energy* **2018**, *9*, 119–130.
10. Xu, Z.G.; Li, J.L.; Zhao, X.M.; Li, L. A review on intelligent road and its related key technologies. *China J. Highw. Transp.* **2019**, *32*, 1–24.
11. Jia, Z.P.; Yang, H.H.; Xie, G.J. A deployment scheme for delay-bounded road side unit in VANET. *J. Xi'an Jiaotong Univ.* **2019**, *53*, 128–135+166.
12. Yeferny, T.; Allani, S. MPC: A RSUs deployment strategy for VANET. *Int. J. Commun. Syst.* **2018**, *31*, e3712. [[CrossRef](#)]
13. Moura, D.L.L.; Cabral, R.S.; Sales, T.; Aquino, A.L.L. An evolutionary algorithm for roadside unit deployment with betweenness centrality preprocessing. *Future Gener. Comput. Syst.* **2018**, *88*, 776–784. [[CrossRef](#)]
14. Chaabene, S.B.; Yeferny, T.; Yahia, S.B. An efficient roadside unit deployment method for vehicular ad-hoc networks. *Procedia Comput. Sci.* **2020**, *176*, 771–780. [[CrossRef](#)]
15. Mao, M.; Yi, P.; Zhang, Z.; Wang, L.; Pei, J. Roadside unit deployment mechanism based on node popularity. *Mob. Inf. Syst.* **2021**, *2021*, 9980093. [[CrossRef](#)]
16. Salari, M.; Kattan, L.; Gentili, M. Optimal roadside units location for path flow reconstruction in a connected vehicle environment. *Transp. Res. Part C Emerg. Technol.* **2022**, *138*, 103625. [[CrossRef](#)]
17. Kui, X.Y.; Du, H.K.; Xiao, X.F.; Li, Y. Traffic amount based road side unit deployment scheme for vehicular network. *J. Cent. South Univ. (Sci. Technol.)* **2016**, *47*, 1573–1579.
18. Xue, L.X.; Yang, Y.C.; Dong, D.C. Roadside infrastructure planning scheme for the urban vehicular networks. *Transp. Res. Procedia* **2017**, *25*, 1380–1396. [[CrossRef](#)]
19. Wang, Y.; Zheng, J. Connectivity analysis of a highway with one entry/exit and multiple roadside units. *IEEE Trans. Veh. Technol.* **2018**, *67*, 11705–11718. [[CrossRef](#)]
20. Mousa, R.J.; Huszák, Á.; Salman, M.A. Enhancing VANET connectivity through a realistic model for RSU deployment on highway. *J. Phys. Conf. Ser.* **2021**, *1804*, 012104. [[CrossRef](#)]
21. Li, Y.; Chen, Z.; Yin, Y.; Peeta, S. Deployment of roadside units to overcome connectivity gap in transportation networks with mixed traffic. *Transp. Res. Part C Emerg. Technol.* **2020**, *111*, 496–512. [[CrossRef](#)]
22. Alheeti, K.; Alaloosy, A.; Khalaf, H.; Alzahrani, A.; Dosary, D.A. An optimal distribution of RSU for improving self-driving vehicle connectivity. *Comput. Mater. Contin.* **2022**, *2*, 3311–3319. [[CrossRef](#)]
23. Ghorai, C.; Banerjee, I. A constrained delaunay triangulation based RSUs deployment strategy to cover a convex region with obstacles for maximizing communications probability between V2I. *Veh. Commun.* **2018**, *13*, 89–103. [[CrossRef](#)]
24. Liu, C.Y.; Huang, H.J.; Du, H.W. Optimal RSUs deployment with delay bound along highways in VANET. *J. Comb. Optim.* **2017**, *33*, 1168–1182. [[CrossRef](#)]
25. Yang, H.H.; Jia, Z.P.; Xie, G.J. Delay-bounded and cost-limited RSU deployment in urban vehicular ad hoc networks. *Sensors* **2018**, *18*, 2764. [[CrossRef](#)]
26. Ahmed, Z.; Naz, S.; Ahmed, J. Minimizing transmission delays in vehicular ad hoc networks by optimized placement of road-side unit. *Wirel. Netw.* **2020**, *26*, 2905–2914. [[CrossRef](#)]
27. Abhishek, N.V.; Aman, M.N.; Lim, T.J.; Sikdar, B. Drive: Detecting malicious roadside units in the internet of vehicles with low latency data integrity. *IEEE Internet Things J.* **2021**, *9*, 3270–3281. [[CrossRef](#)]
28. Massobrio, R.; Toutouh, J.; Nismachnow, S.; Alba, E. Infrastructure deployment in vehicular communication networks using a parallel multiobjective evolutionary algorithm. *Int. J. Intell. Syst.* **2017**, *32*, 801–829. [[CrossRef](#)]
29. Nikookaran, N.; Karakostas, G.; Todd, T.D. Combining capital and operating expenditure costs in vehicular roadside unit placement. *IEEE Trans. Veh. Technol.* **2017**, *66*, 7317–7331. [[CrossRef](#)]
30. Gao, Z.G.; Chen, D.J.; Yao, N.M.; Lu, Z.M.; Chen, B.C. A novel problem model and solution scheme for roadside unit deployment problem in VANETs. *Wirel. Pers. Commun.* **2018**, *98*, 651–663. [[CrossRef](#)]
31. Trullols, O.; Fiore, M.; Casetti, C.; Chiasserini, C.F.; Ordinas, J.M.B. Planning roadside infrastructure for information dissemination in intelligent transportation systems. *Comput. Commun.* **2010**, *33*, 432–442. [[CrossRef](#)]
32. Dubey, B.B.; Chauhan, N.; Pant, S. Effect of position of fixed infrastructure on data dissemination in vanets. *Int. J. Res. Rev. Comput. Sci.* **2011**, *2*, 482–486.
33. Wang, Z.Y.; Zheng, J.; Wu, Y.Y.; Mitton, N. A Centrality-Based RSU Deployment Approach for Vehicular Ad Hoc Networks. In Proceedings of the 2017 IEEE International Conference on Communications, Paris, France, 21–25 May 2017.
34. Coello, C.A.C. Evolutionary multi-objective optimization: A historical view of the field. *IEEE Comput. Intell. Mag.* **2006**, *1*, 28–36. [[CrossRef](#)]
35. Kennedy, J.; Eberhart, R. Particle swarm optimization. In Proceedings of the International Conference on Neural Networks, Perth, Australia, 27 November–1 December 1995.

36. Coello, C.A.C.; Lechuga, M.S. MOPSO: A proposal for multiple objective particle swarm optimization. In Proceedings of the 2002 Congress on Evolutionary Computation, Honolulu, HI, USA, 12–17 May 2002.
37. Sierra, M.R.; Coello, C.A.C. Multi-objective particle swarm optimizers: A survey of the state-of-the-art. *Int. J. Comput. Intell. Res.* **2006**, *2*, 287–308.
38. Sun, J. *Particle Swarm Optimization with Particles Having Quantum Behavior*; Jiangnan University: Wuxi, China, 2009.
39. Knowles, J.D.; Corne, D.W. Approximating the nondominated front using the Pareto archived evolution strategy. *Evol. Comput.* **2000**, *8*, 149–172. [[CrossRef](#)]
40. Deb, K.; Pratap, A.; Agarwal, S.; Meyarivan, T. A fast and elitist multiobjective genetic algorithm: NSGA-II. *IEEE Trans. Evol. Comput.* **2002**, *6*, 182–197. [[CrossRef](#)]
41. Yang, X.S. Multiobjective firefly algorithm for continuous optimization. *Eng. Comput.* **2013**, *29*, 175–184. [[CrossRef](#)]
42. Nguyen, S.; Dupuis, S. An efficient method for computing traffic equilibria in networks with asymmetric transportation costs. *Transp. Sci.* **1984**, *1*, 185–202. [[CrossRef](#)]
43. Zhang, L.L.; Zhao, Q.; Yu, P.; Li, J.; Yao, D.; Wang, X.; Wang, L.; Zhang, L. Research on integrated simulation platform for urban traffic control connecting simulation and practice. *Sci. Rep.* **2022**, *12*, 4536. [[CrossRef](#)] [[PubMed](#)]

Disclaimer/Publisher’s Note: The statements, opinions and data contained in all publications are solely those of the individual author(s) and contributor(s) and not of MDPI and/or the editor(s). MDPI and/or the editor(s) disclaim responsibility for any injury to people or property resulting from any ideas, methods, instructions or products referred to in the content.